High-field remanence properties of synthetic and natural submicrometre haematites and goethites: significance for environmental contexts

B.A. Maher*, V.V. Karloukovski[1], T.J. Mutch

Centre for Environmental Magnetism, Lancaster Environment Centre, Geography Department, Lancaster University, Lancaster LA1 4YB, UK

Abstract

Haematite and goethite are significant magnetic components both of marine and terrestrial sediments. Variable magnetic behaviour in haematite and goethite has been reported, reflecting variations in grain size, crystal defects, nonstoichiometry and mode of formation. Here, we provide new data, first, for a range of synthetic haematite and goethite powders of known grain size and, second, for a variety of haematite- and goethite-bearing natural samples, including red bed samples and modern and fossil soils. Based on the synthetic data, we identify two high-field parameters which may be of value in identifying and characterizing the high-coercivity components of natural environmental samples (even when these are dominated magnetically by the presence of trace concentrations of ferrimagnets). H% indicates the proportion of the room temperature (RT) remanence acquired in fields from 2 Tesla (T) up to 7 T and H_{cool}% indicates the increase or decrease in high-field remanence upon cooling in zero field to 77 K (LT). Used in tandem, these parameters can differentiate between goethite-dominated, and haematite-dominated samples, and indicate differences in haematite grain size. H% values for the synthetic haematites vary between 27% and 38%, with some apparent grain size-dependence, and for the goethites, between 84% and 92%. H_{cool}% values range from +130% to +157% for the goethites and −75% to −95% for those haematites of grain size >100 nm.
© 2004 Elsevier B.V. All rights reserved.

Keywords: haematite; goethite; high-field remanence; environmental magnetism

1. Introduction

Haematite (αFe_2O_3) and goethite ($\alpha FeOOH$), both weakly magnetic, high-coercivity minerals, are formed in terrestrial environments, as a result of oxidative weathering and soil formation—they are the

two most common and abundant iron oxide and oxyhydroxide minerals in soils [1]. Formation of haematite, the most highly oxidized form of iron, is favoured by higher soil temperatures, lower moisture content, lower organic matter content and pH values around 7–8 [1]. Goethite occurs much more widely than haematite and is favoured by moister, more acidic soil conditions. The presence of detrital, aeolian haematite in deep-sea sediments has been identified from high-field magnetic measurements (e.g. [2–4]), X-ray diffraction analysis of magnetic extracts [5] and reflectance spectrophotometry (e.g. [6]). Evidence for the presence of goethite in marine sediments (reported to be equivocal by Schmidt et al. [4]), was presented by Robinson [7] on the basis of Mössbauer spectroscopy. Identification of the fluxes of aeolian-derived haematite and goethite through both time and space is a key environmental task, as it potentially provides information on palaeowinds and changing patterns of aridity and iron supply to the oceans [3,8]. Haematite and goethite have also been recognized as significant magnetic components of various terrestrial sediments, such as the loess sequences of China (e.g. [9]), lacustrine sediments (e.g. [10,11]) and speleothems [12,13].

The magnetic behaviour of haematite and goethite has been reported to be variable, reflecting variations in grain size, crystal defects, nonstoichiometry and mode of formation. In the case of haematite, these complexities gave rise within the palaeomagnetic context to the so-called 'red bed controversy'— whether haematite offers a faithful syn-depositional carrier of natural remanence or a source of poorly constrained, post-depositional remanence due to later authigenesis. In the context of environmental magnetism, non-destructive, magnetic differentiation of these minerals in natural sediments presents the opportunity to identify pedogenic processes, and aeolian sources and pathways. Recent studies have investigated the room and low-temperature remanence properties of natural and synthetic haematites (e.g. [14]), goethites [10,15–17] and maghemitised magnetites [14]. Various methods for identifying haematite and goethite and their relative contributions have been proposed recently, based on a combination of high-field acquisition, orthogonal demagnetisation and cooling and heating of isothermal remanent magnetisation (IRM) [10,11] or on quantitative analysis of IRM components [17], most recently combined with spectroscopic and voltametric analysis [18].

High-coercivity magnetic components have previously been characterized routinely through measurement of a 'high-field isothermal remanence' (HIRM). In the case of many magnetic laboratories, the maximum dc field available for remanence acquisition has been of the order of 1 Tesla (T). The 'HIRM' has thus often been reported as the remanence acquired between either 100 milliTesla (mT) or 300 mT and the 'saturating' field of 1 T (e.g. [19]). However, the value of this parameter has been called into question by recent studies. For example, Liu et al. [14] reported significant IRM acquisition by partially oxidized magnetite at fields in excess of 300 mT; this 'high-field' remanence was not, in fact, magnetically hard but could be demagnetized completely at ac fields of 100 to 300 mT. Further, in the case of goethite, Heller [20] and Rochette and Fillion [16] reported either no or negligible IRM acquisition in applied fields of less than 3 and 4 Tesla (T), respectively. France and Oldfield [10] reported IRM saturation fields of 3 T (and, in one case, 5 T) for synthetic haematites and a variety of soils and sediments, and IRM saturation fields of 2 to >7 T for synthetic goethites and goethite-rich natural samples.

The aims of this study are to study the room temperature (RT) and low temperature (LT) remanence and demagnetization properties of synthetic goethite and haematite samples of known grain sizes, and of natural goethite- and haematite-bearing samples (red beds, soils, and dust-dominated marine sediments), to explore different methods for discriminating between these two minerals in natural samples.

2. Samples and instrumental techniques

2.1. Synthetic samples

Five iron oxide powders (samples G-03, 2087, 8087, Hmt, and FH) were obtained as commercial paint pigments. Analysis by X-ray diffraction (XRD) indicated that samples G-03, 2087, and 8087 consist of pure goethite, and samples Hmt

and FH of haematite (Fig. 1, in the online version of this paper). Their grain sizes were determined from transmission electron micrographs and resultant histograms of grain size distribution (Figs. 2 and 3, in the online version of this paper; Table 1). The haematite grains were observed to be equidimensional, whereas the goethite grains typically display elongate, lath-like morphologies. Two more synthetic haematites (S-04 and S-02) were produced from a fine-grained (50 nm) synthetic magnetite, by heating in air at 500 and 700 °C, respectively, for a period of 4 days. Finally, the finest-grained haematite sample, HM-4, was kindly provided by Dr. H. Stanjek, Institut für Mineralogie und Lagerstättenlehre, Aachen.

2.2. Environmental samples

A range of goethite- and haematite-bearing natural samples, including red beds from the UK, Greenland and Spitsbergen, red soils from the UK and North Africa, goethite-rich modern soils from Brazil [21] and dust-dominated, present day deep-sea sediments [22] was also examined (Table 2). Of the redbed samples, one group of samples from the UK (MS-5 from the Triassic red beds of Devon) was previously reported to contain superparamagnetic (SP) haematite [23]. The N. African (Tunisian and Moroccan) soil samples represent potential source regions for aeolian dust [24]. The goethite-rich soils were obtained in light of previous reports that most

Table 2
Sample information for the natural haematite- and goethite-bearing samples

Sample	Sample code	Description	Source
Red beds	MS-5	Mid Triassic	Sidmouth, S. Devon
	LP-55	Late Triassic	Seven Sisters Bay, S. Wales
	HC-109	Late Triassic	Haven Cliff, Devon
	R-1	Late Triassic	Fleming Fjord Fm., S. Greenland
	WBS-R, WBS-W	Devonian	Wood Bay Series, Spitzbergen
	RBS-V	Devonian	Red Bed Series, Spitzbergen
Red soils	Sampford, GB-4	Valley Farm palaeosol (luvisol)	Barham, East Anglia
	Slapton Bst, Slapton B/C	Modern soil (cambisol)	Slapton, S. Devon
	Tun7, Mor2, Mor3	Modern soils	N. Africa
Goethite-rich soils	US S-03, US S-10, US S-12, US S-40	Goethitic soil	S. Brazil
Dust-dominated deep-sea sediments	K2, K3	Present day sediment off N. Africa	N. Atlantic
Australian sediments	S2-C2, C5, C7, C13, C16	Holocene fen sediment	Caladonia fen, E. Victoria, Australia

soil goethites have particle sizes considerably smaller than ~75 nm [1]. Finally, a number of haematite-bearing Holocene fen sediments, from Victoria, Australia were subjected only to high-field, low-temperature measurements.

2.3. Methods

IRM acquisition experiments were carried out initially at fields of up to 1 T, using an electromagnet (Newport Instruments) and fluxgate spin magnetometer (Molspin). After each acquisition step from 100 mT onwards, the samples were subjected to 100 mT af, using a tumbling Molspin Demagnetizer, and the IRM remaining after this treatment measured. For

Table 1
Mineralogy and grain sizes of synthetic samples

	Sample code	Grain size width/length (nm)	Range (nm)	Grain shape
Synthetic goethites	G-03	55/350	130–260/ 110–710	Acicular
	2087	90/580	20–230/ 180–1010	Acicular
	8087	190/980	30–470/ 190–3080	Acicular
Synthetic haematites	HM-4	25/14		
	S-04	100	50–175	Polyhedral
	Hmt	150	4–350	Polyhedral
	S-02	190	80–420	Polyhedral
	FH	400	130–800	Polyhedral

IRM acquisition experiments at fields >1 T, ~100 mg of each iron oxide powder were tightly wrapped in plastic film and wedged inside 0.5×1.4 cm gelatin capsules. Magnetic remanences were measured in fields from 0 to 7 T and at temperatures between 293 and 77 K (with an accuracy of ~0.5 K) on a single-axis MPMS XL magnetometer (Quantum Design). As the high-coercivity minerals were our primary interest, stepwise acquisition of IRM was performed in fields of 1, 1.5, 2, 3, 4, 5, 6 and 7 T, both at 293 K and 77 K. The magnet was quenched before each IRM measurement; the residual 'zero' field achieved was ~0.1 mT. The thermal behaviour of the room temperature-IRMs acquired at 2 T and at 7 T was monitored whilst cooling samples to 77 K and warming back to 293 K. The temperature dependence of the high-coercivity portion of the IRM ($HIRM_{7-2\ T}$) was then calculated by subtraction of the $IRM_{2\ T}$ from the $IRM_{7\ T}$ curves. This method precludes contribution to the measured remanences of any low-coercivity impurities within the samples (for similar reasons, the low-field susceptibilities were not measured).

3. Results

3.1. Room temperature HIRMs up to 1 T

Fig. 4a (insert) shows the IRM acquisition, in applied fields up to 1 T, by sample Hmt, a pure haematite powder of 150 nm mean grain size. At low fields, there is little evidence of a significant low-coercivity, ferrimagnetic contribution in this sample. It acquires only 7% of its $IRM_{1\ T}$ value by 100 mT and continues to acquire remanence steadily up to 1 T. As expected for SD haematites with high coercivity [25], the sample is not demagnetized with an af treatment of 100 mT (Fig. 4a). However, it is notable that between successive IRM acquisition steps (above 100 mT), some of the HIRM gained is lost upon af demagnetization at 100 mT. As much as ~25% of the $HIRM_{1-0.1\ T}$ is lost upon this treatment. Fig. 4b shows the same experiment for a pure goethite sample (G-03). The concave form of its remanence acquisition curve reflects the recalcitrant nature of its magnetization; the rate of IRM acquisition increasing only at fields beyond 700 mT. At each 100 mT af step, a much smaller proportion (~11%) of the $HIRM_{1-0.1\ T}$ is lost. In contrast, Fig. 4c shows the behaviour of a fully maghemitised ultrafine magnetite powder (MT26, from Maher's original synthetic samples [26]). This (slightly viscous) ferrite sample displayed continued acquisition of IRM above 100 mT and even up to ~300 mT. However, less than 1% of the resultant $HIRM_{1-0.1\ T}$ survived the af treatment. These data thus support Liu et al.'s [14] findings, of some 'high-field' remanence acquisition by such maghemitised ferrites, a remanence which is, however, totally lost upon af treatment.

The synthetic haematite samples, S-02 and S-04 (produced by heating of fine magnetite), also display significant IRM acquisition in low fields. About ~40% of their IRM_{1T} is acquired by 100 mT (Fig. 4d). These data indicate that these synthetic samples consist of a mixture of haematite and a low-coercivity ferrite, probably due to incomplete conversion of the original source material. Consequently, a large proportion of the $HIRM_{1-0.1\ T}$ of these samples was removed by the af demagnetization treatment. Similarly, the synthetic goethite samples, 2087 and 8087, also demonstrate significant IRM acquisition at low fields, again indicating the presence of some ferrite contamination (i.e. at concentrations below the level of detection, ~2%, by XRD). These synthetic mixtures can, however, still be used in our high-field (>1 T) experiments, where the contribution of any low-coercivity components is effectively precluded. The magnetic behaviour of these synthetic mixtures is also of relevance when we consider the low- and high-field IRM behaviour of our range of goethite- and haematite-bearing natural samples. Fig. 4e shows the acquisition of remanence by one of the British red bed samples (LP-55), and Fig. 4f that of one of the red soils (from S. Devon). Whereas all the red bed samples show very little low-field remanence acquisition (they behave very similarly to the synthetic haematite sample shown in Fig. 4a), the soil, in common with all the red and yellow soils examined here, displays behaviour indicative of a mix of low-coercivity ferrites and high-coercivity minerals. Table 2 summarises a range of 'HIRM' measurements for our range of applied fields, both for the synthetic minerals and a representative subset of the natural samples.
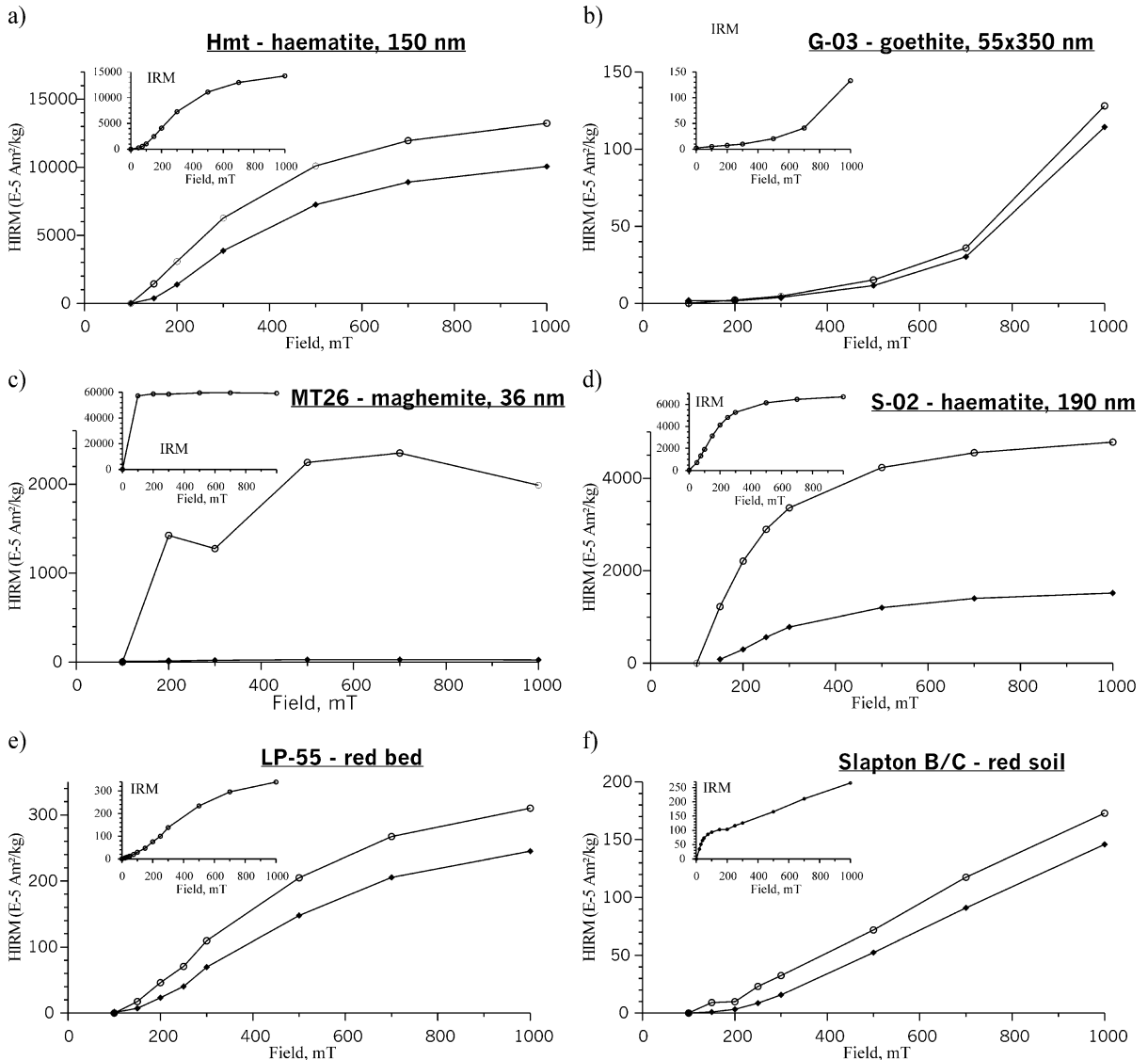
Fig. 4. IRM acquisition curves (shown as inserts) and the stepwise acquisition (open circles) and af demagnetisation (at 100 mT, closed circles) of IRM$_{>0.1 \text{ T}}$ for: synthetic haematites (a, d), goethite (b), maghemite (c) and British red bed (e) and red soil (f).

3.2. Room temperature HIRMs in applied fields up to 7 T

Following the initial 1 T experiments, the MPMS was then used in order to examine the magnetic behaviour of our synthetic and natural samples at significantly higher applied fields. When subjected to fields of up to 7 T, the synthetic goethites exhibited continuous, steady acquisition of IRM (Fig. 5a). The hae-

matites—including both the synthetic powders and the haematite-bearing red bed samples—also continued to acquire remanence up to 7 T, but at a much lower rate (Fig. 5b,c). One way to quantify this contrast in remanence behaviour between the goethites and haematites is to identify the proportion of the total HIRM$_{7-1 \text{ T}}$ that is acquired above 2 T (Fig. 5 and Table 3):

$$H(\%) = (HIRM_{7-2 \text{ T}}/HIRM_{7-1 \text{ T}})*100$$
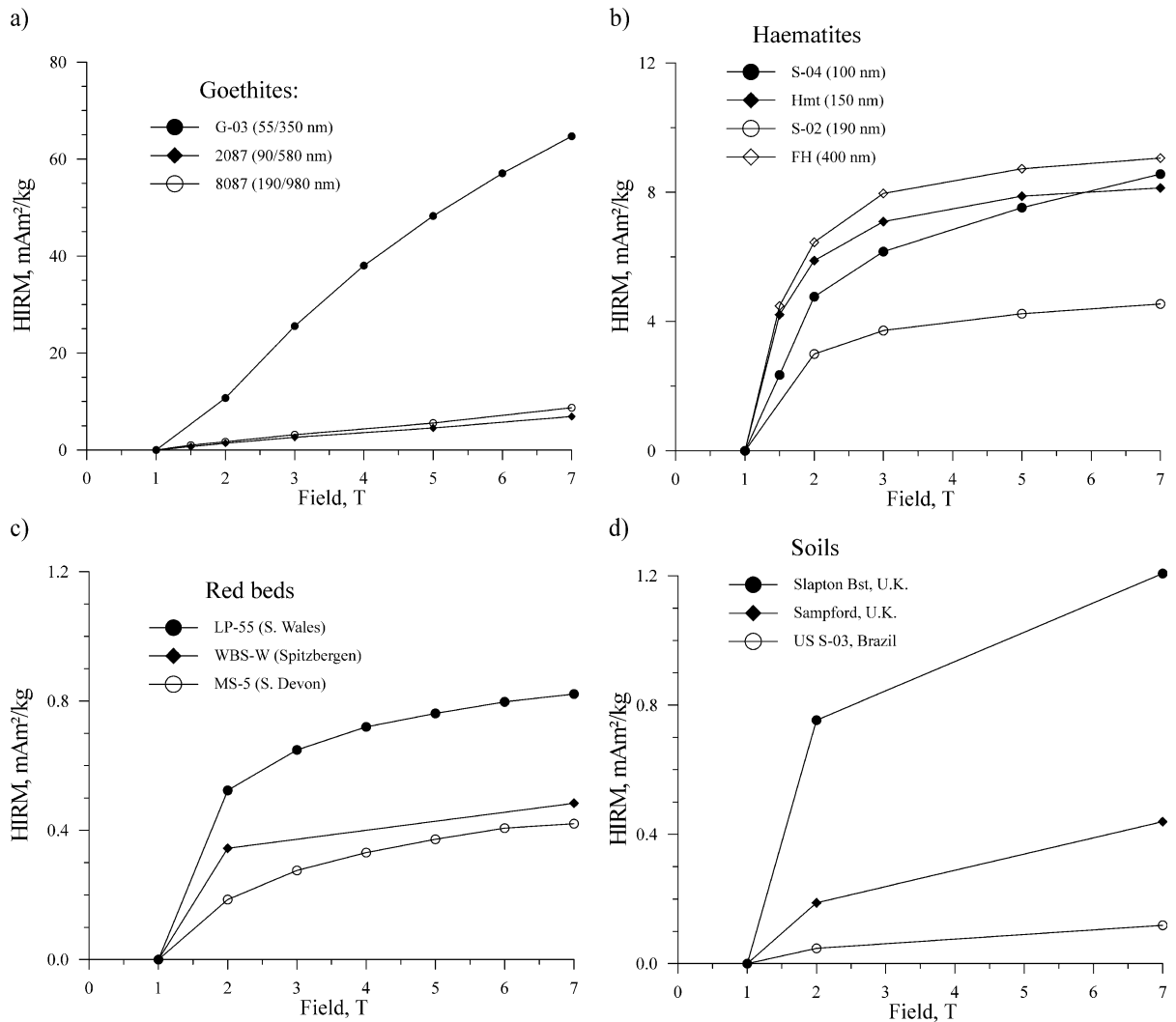
Fig. 5. HIRM$_{>1\ T}$ acquisition in fields up to 7 T; (a) goethites, (b) haematites, (c) red beds, and (d) red and yellow soils.

H% values for the synthetic haematites (Fig. 5b) vary between 27% and 38%, with some apparent grain size-dependence; the coarser the grain size, the smaller is the H% value (Table 3). The goethites (Fig. 5a), on the other hand, maintained or even increased their rate of HIRM acquisition up to 7 T. Their H% values are thus much higher, between 84% and 92%. For our environmental samples, the red beds (Fig. 5c) display H% values of between 31% and 50% (i.e. equal to or higher than those of the synthetic haematites). The high-field acquisition

behaviour of our range of red and yellow soils, shown in Fig. 5d, is characterized by steady acquisition of remanence up to the maximum applied field. Their H % values range widely, from 29% to 60% (Table 3).

3.3. Low-temperature behaviour of room-temperature HIRMs

The low-temperature behaviour of the IRM$_{2\ T}$ and the IRM$_{7\ T}$ acquired at room temperature, and

Table 3
Room temperature HIRM values in fields up to 1 T, and $HIRM_{1-0.1 \, T}$ after af demagnetization at 100 mT

Sample	Mineralogy	$HIRM_{1-0.1 \, T}$ (mAm^2/kg)	$HIRM_{1-0.3 \, T}$ (mAm^2/kg)	$HIRM_{1-0.1 \, T}$ after 100mT af (%)
G-03	g.	1.28	1.23	89.2
2087	g.+f.	0.85	0.14	11.8
8087	g.+f.	3.17	0.88	27.7
HM-4	h.+f.	0.44	0.27	62.3
S-04	h.+f.	120.9	29.9	18.4
Hmt	h.	132.3	69.7	76.0
S-02	h.+f.	47.8	14.2	31.7
FH	h.	109.9	57.3	74.1
MS-5	red bed	1.77	0.66	73.3
LP-55	red bed	3.10	2.00	79.0
WBS-W	red bed	1.79	1.33	91.9
Sampf.	red soil	0.56	0.36	80.8
Slapton Bst	red soil	1.58	1.19	78.1
US S-03	yellow soil	0.32	0.10	37.2
K2	Atlantic sed.	0.93	0.31	39.3

Note the low HIRM values shown by the finest-grained synthetic haematite sample (HM-4), which is below the haematite SP grain size threshold given by Banerjee [33]. g.—goethite, h.—haematite, f.—ferrimagnet.

of the calculated temperature-dependent $HIRM_{7-2 \, T}$, differs markedly for the two sets of synthetics. (We use $HIRM_{7-2 \, T}$ in order to preclude entirely any ferrimagnetic contribution). The behaviour of the $HIRM_{7-2 \, T}$ upon cooling to liquid nitrogen temper-

ature (LT, 77 K) can be described by a parameter, H_{cool} (Fig. 6), as:

$$H_{cool} = (RT \ HIRM_{7-2 \, T} - LT \ HIRM_{7-2 \, T})$$

The normalized version of this parameter, which removes its dependence on the concentration of the high-coercivity contributors, is $H_{cool}\%$:

$$H_{cool}\% = (H_{cool}/RT \ HIRM_{7-2 \, T})*100$$

Upon cooling, each of the synthetic goethites exhibits an almost linear rise in their $HIRM_{7-2 \, T}$, with some apparent dependence on grain size (Fig. 7). The coarsest-grained sample (8087) displays an $H_{cool}\%$ of 130%, whilst that of the finest-grained goethite powder (G-03) is 157% (Table 3).

For the synthetic haematites (Fig. 8), all samples with grain sizes >100 nm exhibit, upon cooling, the Morin transition (T_M) at temperatures between 238 and 241 K. They thus display negative values of $H_{cool}\%$. The Morin transition is a first order magnetic transition in haematites, from a weak ferromagnetic state above T_M (with antiferromagnetic spins lying in the basal plane of the crystal) to an antiferromagnetic state with spins ordered along the c-axis below T_M [27]. The Morin transition was also observed in the cooling HIRM curves of many of our natural, haematite-bearing samples. The Morin transition is observable, for all but the finest-grained synthetic haematite, both in the 2 and 7T IRM runs and in the
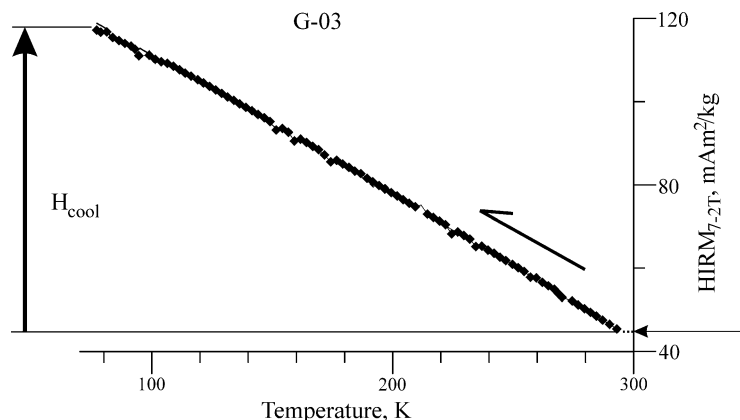

Fig. 6. Low-temperature behaviour of the mass-specific $HIRM_{7-2 \, T}$, illustrating the typical linear rise for goethites, and the new parameter, H_{cool}. The arrow marks the RT value of the $HIRM_{7-2 \, T}$.
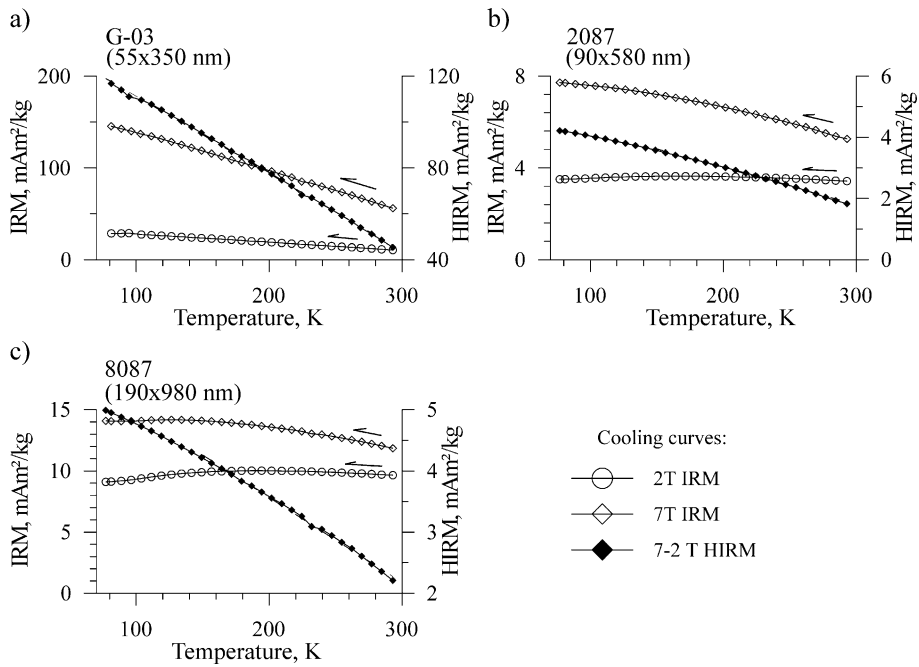
Fig. 7. 2 and 7 T RT IRM cooling curves, from 293 down to 77 K and the calculated HIRM$_{7-2\ T}$ for synthetic goethites. Each sample was subjected to the following sequence of treatments: 2 T at RT; cooling to 77 K; warming to RT; 7 T at RT; cooling to 77 K; warming to RT. Only every third measurement point, at 7.5 K intervals, is shown, for clarity.
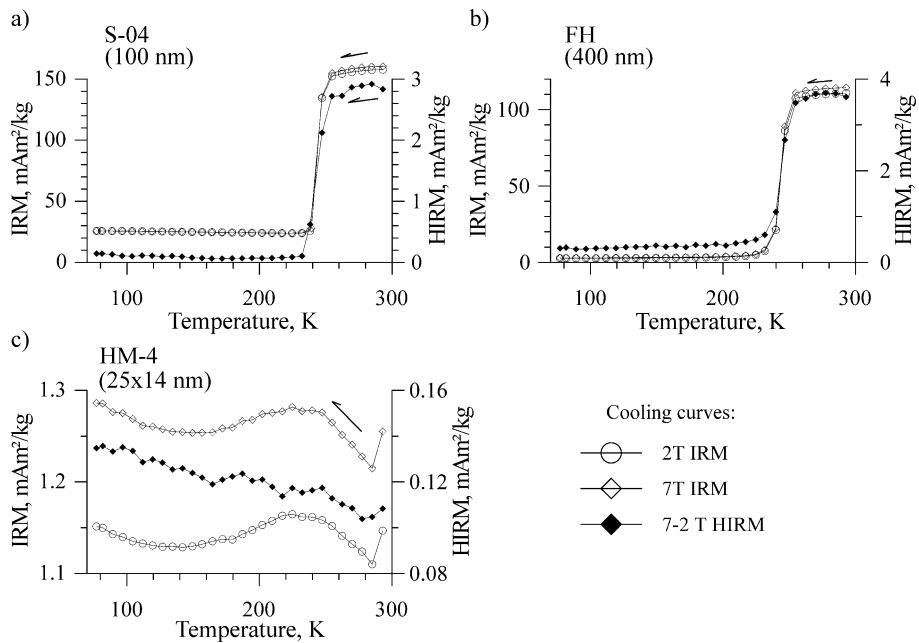

Fig. 8. 2 and 7 T RT IRM cooling curves and HIRM$_{7-2\ T}$ for synthetic haematites.

$HIRM_{7-2\ T}$, giving rise to H_{cool}% values of between −75% and −95% (Table 3; Fig. 8). For the synthetic haematites >100 nm grain size, the temperature of the T_M shows no relationship with grain size, being nearly constant at 238–241 K (Table 4). These values are lower than that—263 K—proposed previously for bulk haematite [28]. Low T_M's (166 K for haematite powders with mean grain diameters of 52.5 nm) were reported by Schroeer and Nininger [29]. However, their haematite powders had been annealed prior to measurement. Our measured T_M values also show no apparent grain size dependence, in contradiction to the relationship proposed by Amin and Arajs [28], again for annealed haematites. An additional possible factor in determining the T_M in haematite is the role of crystal morphology. According to Mossbauer observations, T_M is lower for plate-like and polyhedral haematites (as here), and higher for needle-like and disc-shaped haematites [30].

Our coarser-grained haematite powders display neligible defect moment below T_M [31]: 10% or less of the room temperature HIRM value (Table 5; Fig. 8). The measured defect moment increases with decreasing grain size, to 24% of the room temperature HIRM in sample S-04 (100 nm) and 125% in sample HM-4 (25×14 nm). For the latter sample, the finest-grained of our synthetic haematites, the Morin transition is observable only in the IRM runs, and not in the HIRM. The HIRM displays a slight linear increase upon cooling, thus giving rise to a small but positive H_{cool}% value. Upon cycling back to room temperature, the haematites show varying amounts of

Table 4
Characteristics of the Morin transition in the synthetic haematites

Sample	Size (nm)	T_M (K)	ΔT_M (K)
S-04	100	240	12
Hmt	150	238	21
S-02	190	241	13
FH	400	238	21
HM-4	25×14	146	83

Following Muench et al. [27], the temperature of the transition was defined as that at which a straight line through the steepest part of the transition intersects a straight line through the (defect) antiferromagnetic portion of the curve. The width of the Morin transition, ΔT_M, was determined as the region of deviation of the magnetisation from its smooth pattern before and after T_M [34].

Table 5
Room and low-temperature properties of $HIRM_{7-2\ T}$ for the synthetic haematites and goethites

Sample	Size (nm)	H (%)	$HIRM_{7-2\ T}$			
			at RT (mAm^2/kg)	at LT (mAm^2/kg)	H_{cool} (mAm^2/kg)	H_{cool} (%)
G-03	55×350	83.9	46.31	118.88	72.58	156.7
2087	90×580	91.7	1.88	4.50	2.62	139.2
8087	190×980	85.0	2.28	5.26	2.98	130.4
HM-4	25×14	60.2	0.11	0.14	0.03	27.1
S-04	100	38.4	2.72	0.02	−2.69	−99.2
Hmt	150	27.6	2.81	0.29	−2.52	−89.8
S-02	190	35.1	1.78	0.09	−1.69	−94.7
FH	400	28.1	3.61	0.31	−3.30	−91.5
MS-5		50.1	0.27	0.72	0.46	170.7
MS-5 htd		21.7	0.06	0.05	−0.01	−15.9
LP-55		36.1	0.31	0.70	0.39	126.0
WBS-W		28.9	0.47	0.46	−0.01	−0.6
Sampf.		57.1	0.27	1.37	1.09	399.9
Slapton Bst		37.6	0.45	0.72	0.26	58.1
US S-03		60.0	0.08	0.29	0.22	285.8
K2		55.6	0.13	0.36	0.22	170.2

magnetic memory, recovering between 30 and 50% of their room temperature remanence.

For the natural samples, while the red bed samples from Spitsbergen (Fig. 9d) display the Morin transition in their $HIRM_{2\ T}$, $HIRM_{7\ T}$ and $HIRM_{7-2\ T}$ cooling curves, it is notable that the British redbed samples (Fig. 9a and b) exhibit no Morin transition upon cooling but rather a linear increase in their $HIRM_{7-2\ T}$. This increase is even larger than that shown by our synthetic goethite samples, resulting in positive H_{cool}% values of between 126% and 171%. The question thus arises whether the British redbed samples contain traces of goethite in their otherwise haematite-dominated, high-coercivity fraction. The presence of goethite in redbeds has been reported previously (e.g. [32]) but, on the basis of mixing experiments, France and Oldfield [10] suggested that the goethite:haematite ratio needs to be ~50:1 in order for the Morin transition to be suppressed and the characteristic low-temperature increase in remanence of goethite to be observed. To check for the possible presence of goethite in the redbed samples, a subsample of MS-5 was heated for 25 min., at 350 °C. As a result of this heating, the HIRM increased threefold (Fig. 9c). The previously observed linear increase in $HIRM_{7-2\ T}$ upon cooling disappeared and, instead, signs of a Morin transition appeared, with a
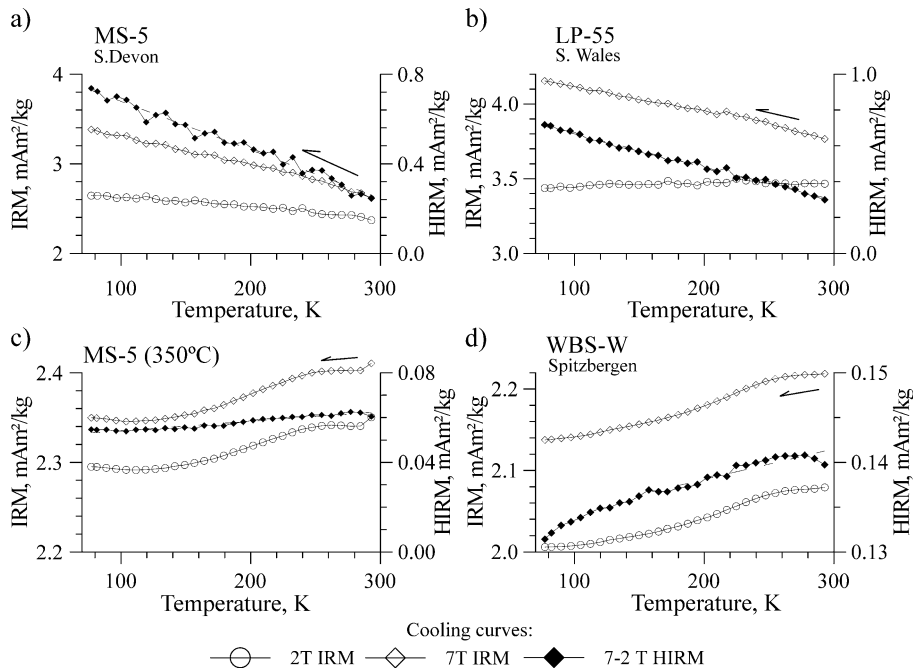
Fig. 9. 2 and 7 T RT IRM cooling curves and HIRM$_{7-2\ T}$ for red beds from Britain and Spitzbergen.

very slight decrease in HIRM$_{7-2\ T}$ upon cooling. These changes in magnetic behaviour upon heating may reflect conversion of an existing goethite component to magnetically stronger but softer haematite and/or possible effective formation of 'larger' haematite grains (e.g. by crystal coalescence [34]). Post-heating, this redbed sample demonstrates somewhat similar magnetic behaviour to the finest-grained synthetic haematite, HM-4 (Fig. 8c).

All the modern and fossil soils, both the red soils from England and Africa and the goethite-rich soils from Brazil, exhibited linear increases, upon cooling, of their original room temperature HIRMs and their HIRM$_{7-2\ T}$ values (Fig. 10). Indeed, the largest H$_{cool}$% value, ~500%, was observed for a reddened palaeosol sample from the UK (Fig. 11).

4. Discussion

Even when the maximum dc field available is of the order of 1 T, the IRM acquisition and demagnetization behaviour of goethites, haematites and maghemitised magnetites is distinctive. As reported previously, each of these mineralogies

displays acquisition of remanence at room temperature in dc fields beyond 0.1 and 0.3 T (albeit at varying rates). The response of each mineral to af demagnetization of the resultant 'HIRM' appears diagnostic. Irrespective of their grain size, the goethites retain most (~90%) of their 'HIRM'; for the haematites, the 'HIRM' loss is as much as ~25%; while the softest, maghemite sample relinquishes virtually all (~99%) of its 'HIRM'. Thus, the mass-normalised HIRM$_{1\ T\ (100\ mT\ af)}$ may provide the simplest means of estimating the remanence contributed by the high-coercivity minerals.

Where it is possible to generate applied dc fields in excess of 1 T, further distinguishing magnetic characteristics can be observed for the high-coercivity minerals. First, due to their pronounced magnetic hardness, the synthetic goethites display higher H % values than do the haematites (although the latter do show some continuing, if minor, IRM acquisition at fields above 2 T). Second, where the change in HIRM$_{7-2\ T}$ upon cooling, H$_{cool}$, shows a linear increase, then this mass-normalised parameter may provide an estimate of the content of goethite and/or ultrafine-grained (<~25 nm) haematite. As previously concluded by France and Oldfield [10], Dekkers [15],
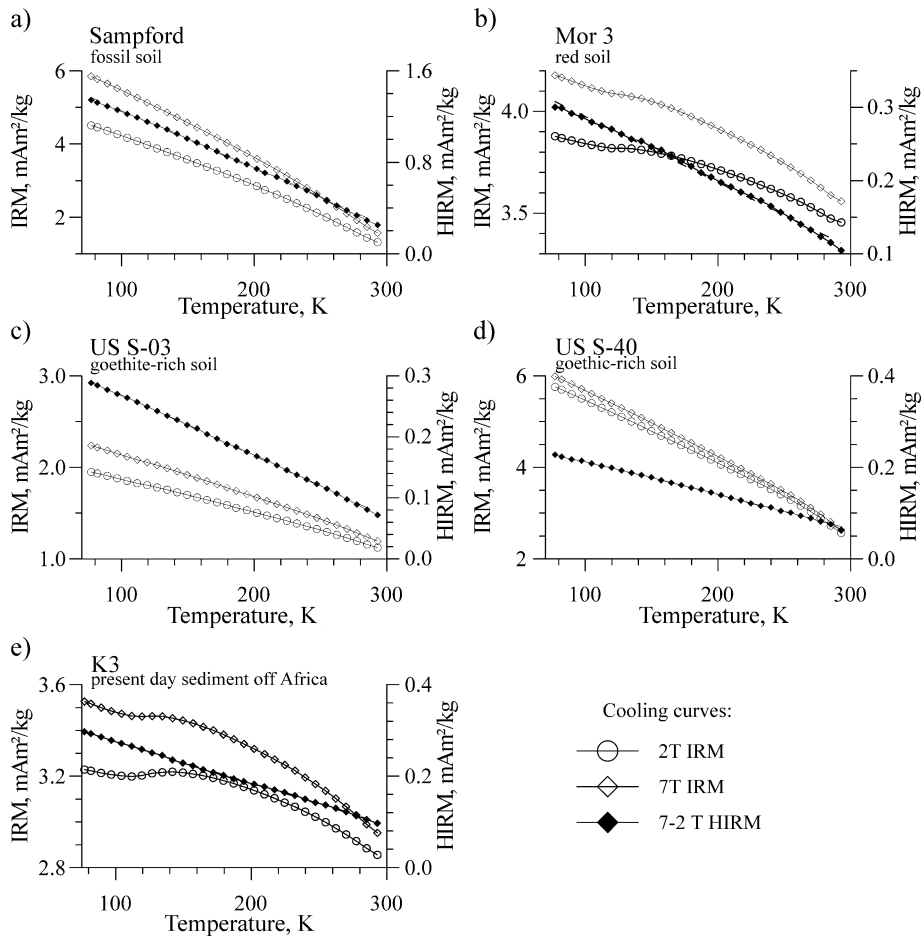
Fig. 10. 2 and 7 T RT IRM cooling curves, from 293 down to 77 K and HIRM$_{7-2 T}$ for a range of red and yellow soils. The Verwey transition in magnetite, at around 120 K, is clearly evident in the IRM curves but is removed in the HIRM curve for the samples shown in (b) and (e).

Rochette and Fillion [16] and Heller [20], monotonic linear increases in IRM upon cooling are displayed by pure goethite samples. Our synthetic goethites displayed H$_{cool}$% values of up to 158%. Dekkers [15] explains such increases in terms of the decreased thermal randomisation of the magnetic moments at low temperature, also pointing out that the strength of the effect is positively (although not linearly) correlated with the degree of aluminium substitution, which may also have the effect of reducing the grain size of the goethite.

Combining our H % parameter and H$_{cool}$% parameter into a single biplot, populated both by our synthetic goethites and haematites and range of haematite- and goethite-bearing natural samples

(Fig. 11), suggests that they can be used as a means of distinguishing the presence of goethite, haematite and SP haematite in environmental samples (even when the latter are dominated magnetically by ferrimagnetic components). The synthetic goethites and the goethite-bearing soils are characterized by moderate to high values of H% and moderate values of H$_{cool}$%, which are always positive. They thus plot mostly to the right of the haematite and haematite-bearing samples. For the synthetic haematites, the coarser-grained samples have lower values of H % and high and negative H$_{cool}$% values. The finer-grained haematites demonstrate suppression of the Morin transition, and so have low but still negative H$_{cool}$% values. The finest haematite powder (25×14
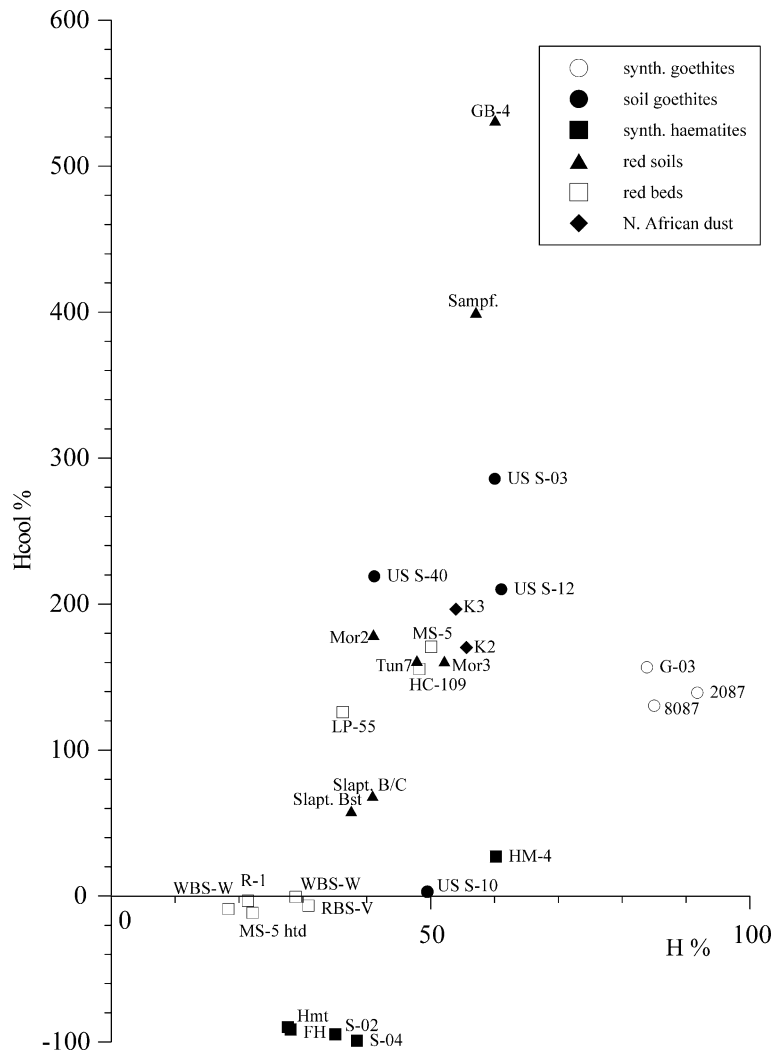
Fig. 11. Biplot of H% versus H_{cool}% for all synthetic and natural samples. The strong viscosity (at 293 K) in the finest synthetic haematite, HM-4, made it difficult to calculate its H% value.

nm) does not display the Morin in its $HIRM_{7-2\ T}$, but instead exhibits a low but positive H_{cool}%. The natural, haematite-bearing samples plot in an apparently systematic line, stretching from the coarsest-grained synthetic haematite (with high, negative H_{cool}% and low H%) to one of the British palaeosol samples (with very high, positive H_{cool}% and higher H%). Along this line, all the redbed samples plot at some distance from the coarsest-grained haematite. The Greenland and Spitsbergen redbed samples fall closest to the finest-grained synthetic haematite, HM-4. Compared with these rocks, the British redbed

samples display higher H_{cool}% values. Extreme H_{cool}% values are shown by two of the reddened fossil soil samples. We suggest that this line indicates changes in haematite grain size. The Greenland and Spitsbergen redbeds would thus be inferred to be close in grain size to our finest-grained synthetic sample (i.e. slightly coarser than ~25 nm), whilst the British redbed samples can be inferred to be of significantly finer grain size. The extreme behaviour of the reddened palaeosol samples suggests they are much finer-grained than any of our other environmental samples, and likely to be approaching the super-

paramagnetic boundary. Either a mix of interacting SP/SD grains or collective magnetic behaviour in truly SP grains could account for the observed remanence characteristics. Hence, we suggest that linear increases in HIRM upon cooling are a feature not only of goethite-bearing samples but also of samples containing ultrafine-grained haematite. To substantiate this suggestion requires investigation of even finer-grained haematite and goethite powders, of controlled grain size (i.e. down to ~8 nm [28]).

Using our H% and H_{cool}% parameters, our ability to differentiate between goethite- and haematite-

dominated materials is hindered only for that central area of the biplot (H% 30–60%; H_{cool}% 150–220%), where the two mineralogies intersect. The modern N. African soils (Tunisia and Morocco) and the present-day, dust-dominated N. Atlantic sediments both fall within this area, as do the British redbed samples. Nevertheless, as shown in Fig. 12, some natural samples locating within this area also span the haematite trend, as demonstrated by our Holocene fen sediments from Australia. We infer from this that these sediments contain haematite covering a range of different grain sizes.
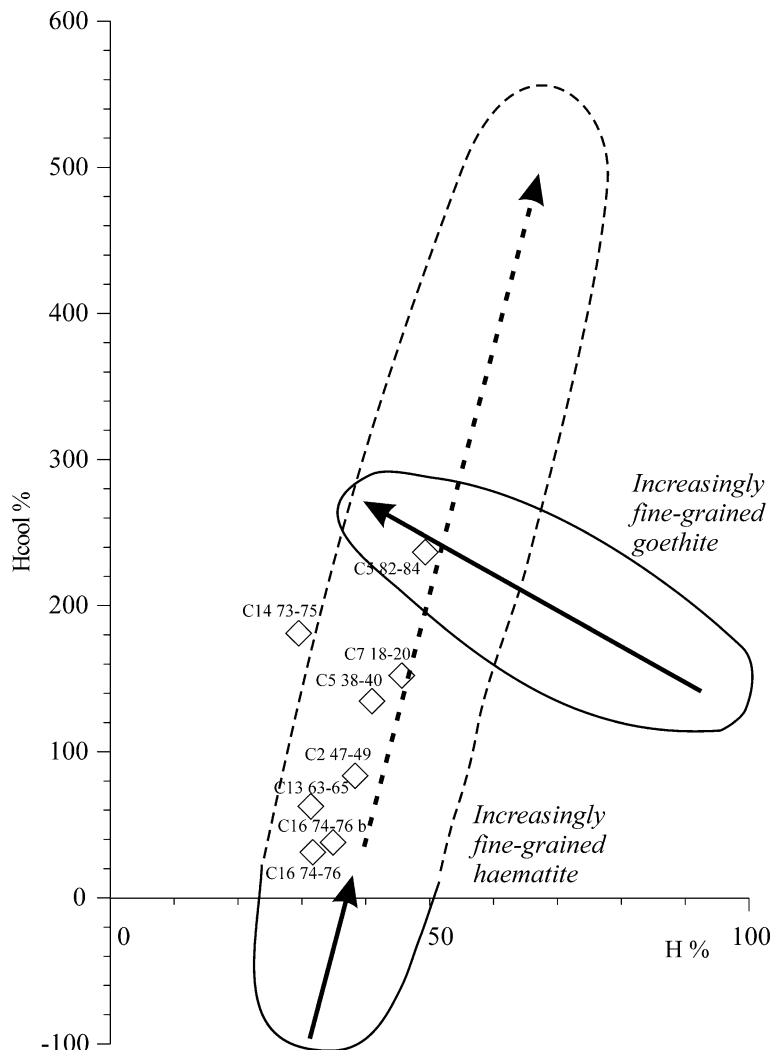

Fig. 12. Biplot of H% versus H_{cool}%, showing envelopes of values for synthetic and natural sample mineralogies, and Australian Holocene fen sediments added. The dashed line indicates the suggested decreasing trend in haematite grain size, towards the SP boundary.

5. Conclusions

(1) Goethite, haematite and maghemitised magnetite each acquire remanence at room temperature in fields beyond 100 mT. Thus, to exclude the possibility of a ferrimagnetic contribution to a 'HIRM'$_{0.1 \text{ or } 0.3 - 1 \text{ T}}$, af demagnetision of the HIRM (at 100 mT af) is required. Goethite is resistant to demagnetization by such treatment. Maghemitised magnetite is completely demagnetized. Intermediate behaviour is shown by haematite, which can lose up to 25% of the remanence acquired at 1 T.

(2) None of our synthetic haematite powders are saturated in a field of 2 T. They continue to acquire remanence in applied dc fields of up to 7 T, although at a much lower rate than that of goethite. The proportion of the total HIRM$_{7-1 \text{ T}}$ acquired above 2 T, the H%, appears to be indicative of the relative proportion of haematite and goethite present in a sample.

(3) Upon cooling the goethites in zero field to 77 K, the HIRM acquired between 2 and 7 T (H$_{cool}$) shows large increases, with some apparent dependence on grain size (i.e. larger increases in smaller grain sizes). Normalising this increase to the original room temperature HIRM$_{7-2 \text{ T}}$, to give the H$_{cool}$%, the synthetic goethites show positive values of up to 158%.

(4) Polyhedral, non-annealed haematites, larger than 100 nm, display a Morin transition at the relatively low temperature of ~240 K, with no apparent dependence on grain size. Their H$_{cool}$% values range from −75% to −95%.

(5) Ultrafine synthetic haematite grains, of ~25 nm grain size, do not show the Morin transition in their HIRM$_{7-2 \text{ T}}$.

(6) A range of natural, haematite- and goethite-bearing samples, including redbeds and modern and fossil soils, display H% values ranging from 30% to 60%, and, with the exception of the non-British redbeds, positive H$_{cool}$% values ranging from 140% to 500%. The Spitsbergen and Greenland redbed samples display the Morin transition upon cooling and thus have negative H$_{cool}$% values.

(7) From the behaviour of both the synthetic and haematite-bearing samples, linear increases in HIRM upon cooling appear to be a feature not only of goethite-bearing samples but also of samples containing ultrafine-grained haematite.

(8) In combination, it may be possible to use the H% and the H$_{cool}$% parameters to distinguish the presence of goethite, haematite, and haematite of grain size close to the superparamagnetic boundary, in a range of different environmental materials (soils, sediments, rocks). Such information is of key environmental value, especially in identifying the sources of aeolian and other terrigenous inputs to the deep-sea sedimentary record.

Appendix A. Supplementary data

Supplementary data associated with this article can be found, in the online version, at doi:10.1016/ j.epsl.2004.05.042.

References

[1] U. Schwertmann, R.M. Taylor, Miner. Soil Environ. (1989).

[2] J.C. Larrasoaña, A.P. Roberts, E.J. Rohling, M.W. Winklhofer, R. Wehausen, Three million years of North Saharan dust supply into the eastern Mediterranean Sea, Climate Dynamics (in press).

[3] B.A. Maher, P.F. Dennis, Evidence against dust-mediated control of glacial-interglacial changes in atmospheric CO_2, Nature 411 (2001) 176–180.

[4] A.M. Schmidt, T. von Dobeneck, U. Bleil, Magnetic characterization of Holocene sedimentation in the South Atlantic, Palaeoceanography 14 (1999) 465–481.

[5] M.W. Hounslow, B.A. Maher, Source of the climate signal recorded by magnetic susceptibility variations in Indian Ocean sediments, J. Geophys. Res. 104 (1999) 5047–5061.

[6] W.L. Balsam, B.C. Deaton, Sediment dispersal in the Atlantic Ocean—evaluation by visible light spectra, Aquat. Sci. 4 (1991) 411–447.

[7] S.G. Robinson, The late Pleistocene palaeoclimatic record of North Atlantic deep-sea sediments revealed by mineral–magnetic measurements, Phys. Earth Planet. Int. 42 (1986) 22–47.

[8] J.H. Martin, Glacial–interglacial CO_2 change; the iron hypothesis, Paleoceanography 5 (1990) 1–13.

[9] B.A. Maher, R. Thompson, Palaeomonsoons I: the magnetic record of palaeoclimate in the terrestrial loess and palaeosol sequences, in: B.A. Maher, R. Thompson (Eds.), Quaternary Climates, Environments and Magnetism, Cambridge University Press, Cambridge, 1999, pp. 81–125.

[10] D.E. France, F. Oldfield, Identifying goethite and haematite from rock magnetic measurements of soils and sediments, J. Geophys. Res. 105 (2000) 2781–2795.

[11] M.F. Bogalo, F. Heller, M.L. Osete, Isothermal remanence experiments at room and at liquid nitrogen temperature: application to soil studies, Geophys. Res. Lett. 28 (2001) 419–422.

[12] V. Rusanov, R.G. Gilson, A. Lougear, A.X. Trautwein, Mossbauer, magnetic, X-ray fluorescence and transmission electron microscope study of natural magnetic materials from speleothems: haematite and the Morin transition, Hyperfine Interact. 128 (2000) 353–373.

[13] M. Noel, Palaeomagnetic and archaeomagnetic studies in caves of Guangxi, Cave Sci. 17 (1990) 73–76.

[14] Q. Liu, S.K. Banerjee, M.J. Jackson, R. Zhu, Y. Pan, A new method in mineral magnetism for the separation of weak antiferromagnetic signal from a strong ferrimagnetic background, Geophys. Res. Lett. 29 (2002) 6-1-4.

[15] M.J. Dekkers, Magnetic properties of natural goethite: I. Grain size dependence of some low and high field related rock magnetic parameters measured at room temperature, Geophys. J. 97 (1989) 323–340.

[16] P. Rochette, P.G. Fillion, Field and temperature behaviour of remanence in synthetic goethite: palaeomagnetic implications, Geophys. Res. Lett. 16 (1989) 851–854.

[17] P.P. Kruiver, M.J. Dekkers, D. Heslop, Quantification of magnetic coercivity components by the analysis of acquisition curves of isothermal remanent magnetisation, Earth Planet. Sci. Lett. 189 (2001) 269–276.

[18] T. Grygar, J. Dedecek, P.P. Kruiver, M.J. Dekkers, P. Bezdicka, O. Schneeweiss, Iron oxide mineralogy in late Miocene red beds from La Gloria, Spain: rock-magnetic, voltametric and Vis spectroscopy analyses, Catena 53 (2003) 115–132.

[19] R. Thompson, F. Oldfield, Environmental Magnetism, Allen & Unwin, London, 1986, 227 pp.

[20] F. Heller, Rock magnetic studies of Upper Jurassic limestones from southern Germany, J. Geophys. 44 (1978) 525–543.

[21] U. Schwertmann, N. Kampf, Properties of goethite and hematite in kaolinitic soils of southern and central Brazil, Soil Sci. 139 (1985) 344–350.

[22] S.J. Watkins, B.A. Maher, Magnetic characterisation of present day deep-sea sediments and sources in the North Atlantic, Earth Planet. Sci. Lett. 214 (2003) 379–394.

[23] K.M. Creer, Superparamagnetism in red sandstones, Geophys. J. R. Astron. Soc. 5 (1961) 16–28.

[24] T.J. Mutch, Magnetic properties of Quaternary deep-sea sediments: use as proxies for dust inputs? Unpublished PhD thesis, University of East Anglia, 2002.

[25] D.J. Dunlop, Magnetic properties of fine-particle hematite, Ann. Geophys. 27 (1971) 269–293.

[26] B.A. Maher, Magnetic properties of some synthetic submicron magnetites, Geophys. J. R. Astron. Soc. 94 (1988) 83–96.

[27] G.J. Muench, S. Arajs, E. Matjevic, The Morin transition in small α-Fe_2O_3 particles, Phys. Status Solidi 92 (1985) 187–192.

[28] N. Amin, S. Arajs, Morin temperature of annealed submicronic α-Fe_2O_3 particles, Phys. Rev. B 53 (1987) 4810–4811.

[29] D. Schroeer, R.C. Nininger, Morin transition in α-Fe_2O_3 microcrystals, Phys. Review Lett. 19 (1967) 632–634.

[30] M. Sorescu, R.A. Brand, D. Mihaila-Tarabasanu, L. Diamandescu, The crucial role of particle morphology in the magnetic properties of haematite, J. Appl. Phys. 85 (1999) 5546–5548.

[31] T.E. Gallon, The remanent magnetization of haematite single crystals, Proc. R. Soc. Lond. A303 (1968) 511–524.

[32] C.B. de Boer, Rock magnetic studies on hematite, maghemite and combustion-metamorphic rocks, Unpublished PhD thesis, University of Utrecht, 1999.

[33] S.K. Banerjee, New grain size limits for palaeomagnetic stability in haematite, Nat. Phys. Sci. 232 (1971) 15–16.

[34] M. Vasquez-Mansilla, R. Zysler, D. Fiorani, L. Suber, Annealing effects on magnetic properties of acicular hematite nanoparticles, Physica B 320 (2002) 206–209.